Semi-empirical approach to the simulation of molecule-surface reaction dynamcis

Migliorini, D.

Chapter 4

Surface Reaction Barriometry: Methane Dissociation on Flat and Stepped Transition Metal Surfaces

This Chapter is based on:

D. Migliorini[1], H. Chadwick[1], F. Nattino, A. Gutiérrez-González, E. Dombrowski, E. A. High, H. Guo, A. L. Utz, B. Jackson, R. D. Beck, and G. J. Kroes, *J. Chem. Phys. Lett.*, 8, 4177 (2017); (E) *J. Chem. Phys. Lett.*, 10, 661 (2019)

https://pubs.acs.org/doi/abs/10.1021/acs.jpclett.7b01905

(E) https://pubs.acs.org/doi/abs/10.1021/acs.jpclett.9b00186

which are reproduced with the permission of ACS Publications[2].

[1]These authors contributed equally to the paper.

[2]further permissions related to the material excerpted should be directed to the ACS.

Abstract

Accurately simulating heterogeneously catalyzed reactions requires reliable barriers for molecules reacting at defects on metal surfaces, such as steps. However, first principles methods capable of computing these barriers to chemical accuracy have yet to be demonstrated. In this Chapter we show that state-resolved molecular beam experiments combined with *ab initio* molecular dynamics using specific reaction parameter density functional theory (SRP-DFT) can determine the molecule-metal surface interaction with the required reliability. Crucially, SRP-DFT exhibits transferability: the functional devised for methane reacting on a flat (111) face of Pt (and Ni) also describes its reaction on stepped Pt(211) with chemical accuracy. Our approach can help bridge the materials gap between fundamental surface science studies on regular surfaces and heterogeneous catalysis in which defected surfaces are important.

4.1 Introduction

Heterogeneous catalysis plays a key role in the production of most chemicals, and quantitatively accurate predictions of the rates and pathways of elementary steps can guide catalyst design and optimization. With the theoretical toolbox now available, it is possible to predict trends in transition-metal catalysis, and identify which materials should constitute good catalysts for making particular chemicals [1]. However, theory still struggles to compute reaction rates reliably, with errors in the rate of ammonia production over Ru still being approximately 1-2 orders of magnitude [2].

Several factors complicate the calculation of rates of heterogeneously catalyzed processes [3]. These processes typically consist of sequences of elementary surface reactions, as illustrated by the Haber-Bosch production of NH_3 in work that contributed to G. Ertl winning the 2007 Nobel Prize in chemistry [4]. Typically, only one or a few reactions are "rate-controlling", so one can focus on these reactions [5]. However, the exponential dependence of reaction rate on activa-

tion energy places severe demands on the accuracy of reaction barrier heights calculated for the associated rate-controlling transition states [3, 6]. These barrier heights cannot be measured directly, and are best determined through a close comparison of molecular beam experiments and dynamics calculations reproducing the reaction probabilities measured therein [7]. On the theory side, first principles methods capable of computing the electronic energies of these states with chemical accuracy (1 kcal/mol) have yet to be demonstrated, and efforts to develop databases of reaction barriers for surface reactions are in their infancy [7]: Presently chemically accurate barriers are available only for four systems, in which a molecule reacts with a flat, low index metal surface [7–10].

While a semi-empirical density functional theory (DFT) approach [10, 11] for computing barriers on flat surfaces has been demonstrated, it has long been known [12] that catalyzed reactions proceed mainly over sites usually called "defects", such as kinks and steps [13–16]. Simulations of catalyzed reactions often attempt to take this into account by computing the energies of the relevant states for model "defected surfaces" using standard density functionals [6, 17, 18]. Here, by defected surface we mean a surface containing line defects (such as steps or edges) or point defects (such as kinks or corners), even though such a surface might be a regular crystal surface definable through Miller indices. Unfortunately, such simulations cannot yet be expected to capture the important effects of point and extended surface defects and of multifaceted surfaces [3]. Furthermore, standard density functionals (i.e., the classes of non-empirical functionals based on constraints and semi-empirical functionals fitted to a range of chemical and/or material properties [3]) only yield semi-quantitative results for barrier heights of surface reactions on metals [7].

Here, we test the accuracy of a joint theoretical-experimental approach (which we call reaction barriometry) that uses results from a flat, low index metal surface to obtain the minimum barrier for a molecule (CHD_3) reacting on a stepped Pt(211) surface. We apply a surface science approach to derive a semi-empirical functional that accurately describes a reaction on a flat metal surface (CHD_3 + Pt(111)), and then rely on the transferability of that functional to describe

the reaction on the defected surface (Pt(211), note that (211) surfaces of fcc metals consist of 3-atom wide (111) terraces and (100) steps). For catalysis by Pt-particles, the molecule-surface reaction we address is the rate-limiting step of the steam-reforming process [19], which is widely used for industrial hydrogen production. Microkinetic simulations of steam reforming on Ni (the commercial catalyst) and Pt often use the (211) surface to simulate step site reactivity [6, 18]. Dissociation of methane on transition metal surfaces is also of fundamental interest, as a benchmark system exhibiting several interesting dynamical features [20–22], including selective bond breaking of partially deuterated methane [23].

This Chapter is organized as follows. The method used to perform and analyze the calculations is reported in Section 4.2, the main results and their implications for heterogeneous catalysis are then discussed in Section 4.3 and the conclusions are summarized in Section 4.4.

4.2 Method

Our approach for determining barriers for molecules reacting at defected surfaces can be summarized in five steps (extensively discussed in Chapter 2 and Refs. [10, 24]): (i) Perform conventional ("laser-off") molecular beam experiments on the molecule (here: CHD_3) reacting on a flat surface (here: Pt(111), top view in Figure 4.1A) to determine the reaction probability as a function of average incident kinetic energy, $\langle E_i \rangle$. In these experiments, the $\langle E_i \rangle$, the nozzle temperature T_n, and the surface temperature T_s should be taken such that the applicability of classical mechanics is ensured. Next, (ii) fit a candidate specific reaction parameter (SRP) functional to the measured reaction probabilities (S_0) using *ab initio* molecular dynamics (AIMD) calculations. Subsequently (iii) measure the initial state-resolved reaction probabilities (here: for $CHD_3(\nu_1 = 1)$), and (iv) validate the candidate SRP functional by showing that AIMD calculations using this functional also reproduce the initial state-resolved experiments. The new finding presented here is that, in the final step (v), the SRP density functional derived for the molecule interacting with the flat surface can be used to derive

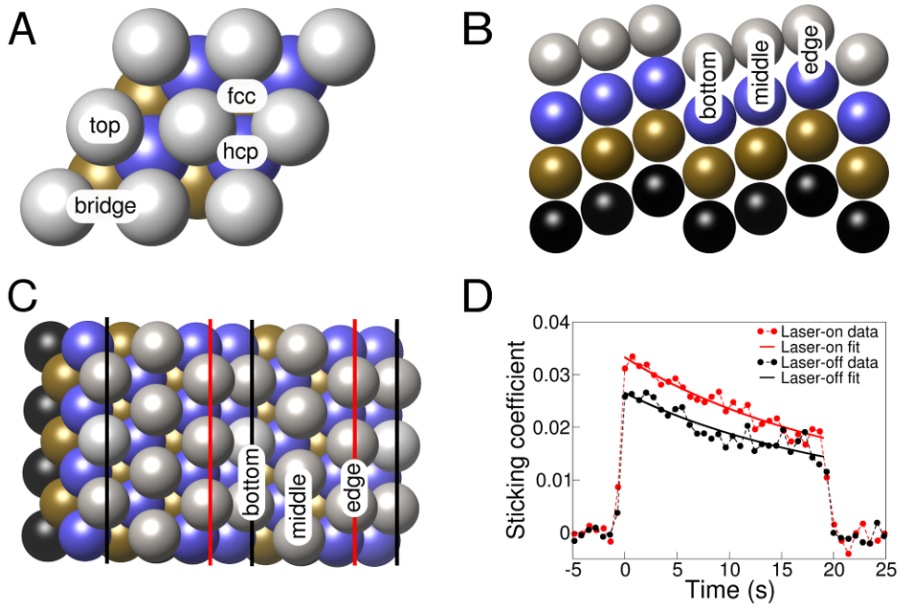

Figure 4.1: Views of the (111) and the (211) faces of fcc metals (like Ni and Pt), and experimental Kings and Well trace. (A) Top view of the (111) face. (B and C) Side and top views of the (211) face. (D) Kings and Wells trace of a measurement on CHD_3 + Pt(111) at $\langle E_i \rangle = 82$ kJ/mol.

the barrier height for the molecule reacting on the defected (stepped) surface, as we will show here for CHD_3 + Pt(211) (top and side views in Figures 4.1B and 4.1C). The underlying assumption, which has been argued before [10, 11], is this: if an SRP functional provides chemically accurate predictions of S_0 for measurements made near the energy threshold and for multiple combinations of $\langle E_i \rangle$ and vibrational excitation (laser-off or $\nu_1 = 1$ reaction), it will also provide a chemically accurate description of the height of the minimum barrier, and accurately describe its geometry. All experiments and calculations reported here were done for normal incidence. As the dissociation of methane on transition metal surfaces like Ni(111) [25] and Pt(111) [26] typically follows normal energy scaling, this samples the initial conditions which have the most significant effect on the reactivity.

In modeling the reaction of methane with transition metal surfaces we compute reaction probabilities with AIMD, which allows modeling of the effects of

surface atom vibrations and T_s, as required [27]. The calculations use the *ab initio* total energy and AIMD program VASP [28, 29]. The SRP functional derived previously [10] for CHD_3 + Ni(111) is:

$$E_{XC}^{SRP} = x \cdot E_X^{RPBE} + (1 - x) \cdot E_X^{PBE} + E_C^{\text{vdW-DF}}. \tag{4.1}$$

In Equation 4.1 (for detailed justification see Refs. [10, 24] and Chapter 2), E_X^{RPBE} and E_X^{PBE} are the exchange parts of the RPBE [30] and PBE [31] functionals, and $E_C^{\text{vdW-DF}}$ is a correlation functional that provides an approximate description of the attractive van der Waals interaction [32]. Adjusting the fit parameter x allows one to reproduce reactivity [10], while the use of well-constrained exchange and correlation functionals ensures the functional's robustness for other system properties, e.g. crystal lattice structure. As before [10], molecular beam reflectivity experiments [33] are used to determine CHD_3 sticking coefficients, with typical data shown in Figure 4.1D. Laser preparation of the incident CHD_3 in a specific rovibrationally excited quantum state ($\nu_1 = 1$, $J = 2$, $K = 1$) yields state-resolved reaction probabilities of $CHD_3(\nu_1 = 1)$. For further methodological details, see Chapter 2 and the SI of Ref. [24].

4.3 Results and Discussion

4.3.1 Theory-Experiment Comparison

To enable us to make an important point regarding the transferability of our approach, reaction probabilities computed and measured earlier for CHD_3 + Ni(111) are presented in Figure 4.2A.

For CHD_3 + Ni(111), the value of x (0.32) was fitted with AIMD calculations modeling laser-off experiments with $\langle E_i \rangle$ = 112 and 121 kJ/mol (T_n = 600 and 650 K). Using that x value, AIMD calculations predicted S_0 for $CHD_3(\nu_1 = 1)$ with chemical accuracy, confirming the quality of the SRP functional (Figure 4.2A). For $\langle E_i \rangle > 130$ kJ/mol calculations slightly overestimated laser-off reactivity. This was attributed to quasi-classical mechanics overestimating the reac-

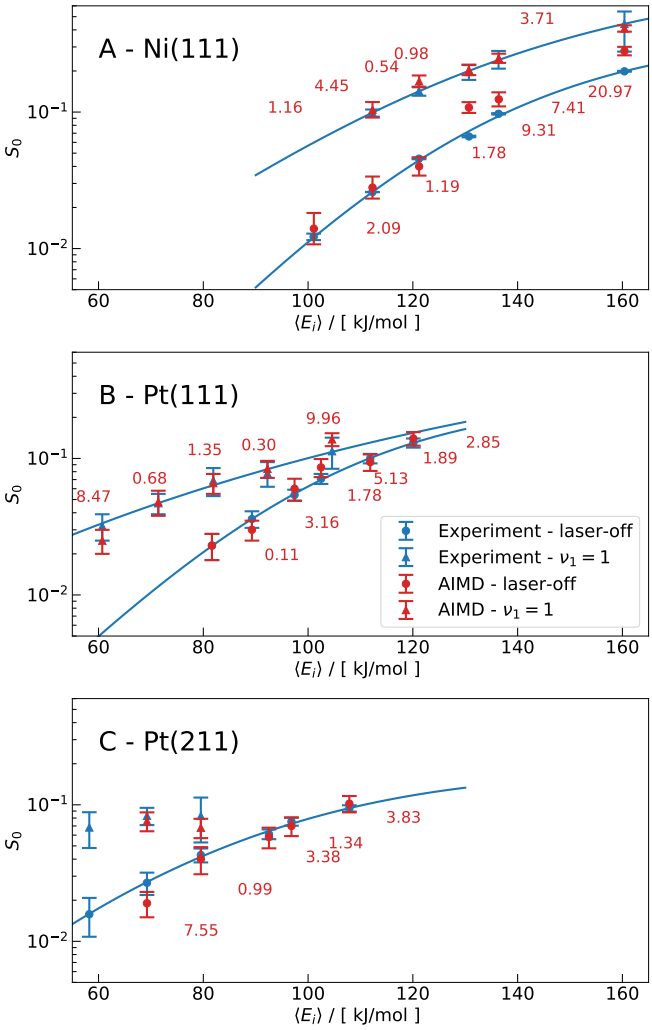

Figure 4.2: Comparison of theory with experiments for CHD_3 + Ni(111), Pt(111), and Pt(211): Reaction probabilities as a function of $\langle E_i \rangle$. (A) Reaction probabilities calculated with AIMD and measured in molecular beam experiments for CHD_3 + Ni(111). Blue symbols and lines: experimental results and fits to experiment. Red symbols: AIMD results. Circles are for laser-off conditions and triangles for $\nu_1 = 1$ CHD_3. Numbers show the distance of the computed reaction probability to the fitted experimental curve along the incidence energy axis, in kJ/mol. Results reported in Panel A are reproduced from Ref. [10]. (B and C) Same as Panel A, but results from this Chapter for CHD_3 + Pt(111) and Pt(211).

tivity of excited CD vibrational states, which become increasingly populated at higher T_n ($\geq$ 700 K). Under these conditions AIMD calculations overestimate the fraction of CHD_3 molecules dissociating via CD bond cleavage [10]. Here, new experiments and AIMD calculations are performed for CHD_3 + Pt(111). In the fitting of x in Equation 4.1 we could take a shortcut as the value of $x = 0.32$ derived for CHD_3 + Ni(111) also provided excellent agreement between experiment and theory for CHD_3 + Pt(111) (Figure 4.2B). For laser-off reaction chemical accuracy is obtained over the entire range of $\langle E_i \rangle$: on average the distance between the computed reaction probabilities and the fitted experimental curve along the energy axis is less than 4.2 kJ/mol ($\approx$ 1 kcal/mol). The minimum barrier height to reaction, calculated with the surface frozen in its relaxed 0 K configuration, on Pt(111) (E_b = 79 kJ/mol, Table 4.1) is considerably lower than on Ni(111) (98 kJ/mol, Table 4.1). Therefore, laser-off experiments with $\langle E_i \rangle \leq$ 120 kJ/mol ($T_n \leq$ 650 K) sample the full reactivity range of interest on Pt(111), and the complications associated with excited CD vibrational states at higher T_n seen for Ni(111) are avoided. The AIMD results also show chemical accuracy for $CHD_3(\nu_1 = 1)$ + Pt(111), a result that is not achieved using the PBE functional [34] despite the transition state being similar to the SRP functional, as shown in Table 4.1 and discussed in Chapter 6. We attribute the observation of larger individual deviations to statistical fluctuations in the calculated reaction probabilities, and we note that in two of the three cases, computed probabilities are compared to an extrapolated ($\nu_1 = 1$) experimental curve. The comparison of the AIMD results to the molecular beam data also meets a statistical accuracy test (see Table S1 and the SI of Ref. [24]).

The good agreement observed here for CHD_3 + Pt(111) using an SRP functional developed for CHD_3 + Ni(111) suggests that SRP functionals are transferable among chemically related systems (here: systems in which the same molecule reacts on the same low index surface of group 10 metals). We take this as additional proof of the sound physical basis of the SRP-DFT approach. We now proceed to CHD_3 reacting on the stepped Pt(211) surface. Again, the agreement between theory and experiment is excellent (Figure 4.2C). The theory using

metal surface	E_b / [kJ/mol]	r_b / [Å]	Z_b / [Å]	θ_{CH} / [∘]
Ni(111)	97.9 (104.2)	1.61 (1.60)	2.18 (2.12)	136 (133)
Pt(111)	78.7 (77.8)	1.56 (1.50)	2.28 (2.25)	133 (134)
Pt(211)	53.9 (46.0)	1.53 (1.48)	2.27 (2.24)	133 (134)

Table 4.1: Computed barrier heights E_b, the CH distance of the dissociating bond r_b, the distance of the C atom to the surface Z_b, and the angle the dissociating bond makes with the surface normal (θ_{CH}) in the minimum barrier geometry for the SRP functional. PBE results (from Ref. [35] for Ni(111), Ref. [36] for Pt(111), and from this work for Pt(211)) are shown in brackets for comparison.

$x = 0.32$, describes the measured laser-off reactivity with chemical accuracy. Not enough data were available to make a fit of the experimental data for $\nu_1 = 1$ reaction, but the theoretical reaction probabilities agree with the experimental values within error bars. Again, the comparison of the AIMD results to the molecular beam data also meets our statistical accuracy test (Table S1 in the SI of Ref. [24]). Note that we were not able to compare experiment with AIMD calculations at the lowest $\langle E_i \rangle$ for which experimental results were available. For this condition, large calculated trapping probabilities precluded an accurate comparison of the AIMD results with the experiments (see Figure 4.3). However, this does not invalidate our comparison since the average trapping time on the surface has been estimated using Frenkel's formula [37] to be about 43 ps. In this long trapping time the molecule has time to explore the surface and to react on higher order defects (such as kinks) that might be present on the experimental surface possibly reducing the difference between experiments and theory (more details are reported in Chapter 5). Furthermore, at higher $\langle E_i \rangle$ where the trapping probability is negligible, the agreement with the experiments is excellent. The E_b value extracted for CH_4 + Pt(211) (54 kJ/mol, Table 4.1) is much lower than for Pt(111) (79 kJ/mol).

The AIMD calculations also yield insights into reaction dynamics. Figure 4.4 shows that even vibrationally pre-excited CHD_3 reacts preferentially at the steps (near the under-coordinated Pt atoms labeled "edge" in Figures 4.1B and 4.1C). This prediction can be tested with reflection absorption infrared spectroscopy

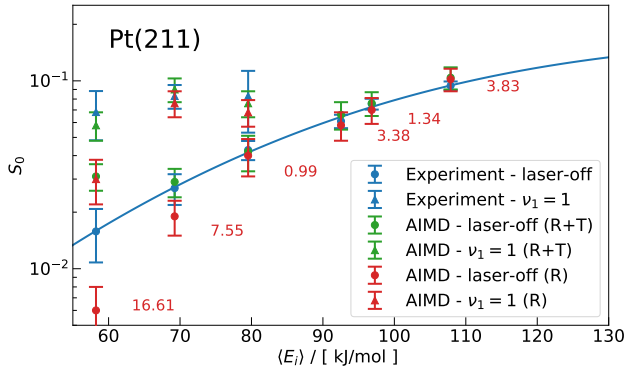

Figure 4.3: Experimental and AIMD results (blue and red, respectively) for CHD_3 on Pt(211). The AIMD results computed considering the trapped trajectories as reacted (R+T) are reported in green. The distance from the AIMD results to the experimental fit (in kJ/mol) is reported in red.

[38]. While approaching the surface at normal incidence, the reactive molecules hardly change their projection on the surface (Figure 4.4). This result simplifies high-dimensional quantum dynamics calculations, because the dimensionality can be reduced using the "sudden" approximation to the molecule's motion along the surface. This amounts to averaging over calculations performed for fixed projections of the molecule on the surface [39–41]. Finally, calculations on CHD_3 + Pt(111) using the reaction path Hamiltonian (RPH) method [39] reveal how the molecular physisorption well affects reactivity. As discussed in the SI of Ref. [24], according to RPH calculations the use of the SRP functional yields a larger promoting effect on the reaction of pre-exciting the CH- and CD-stretch vibrations than the use of the PBE functional (see Figure S2 and the SI of Ref. [24]). Model calculations attribute this to the molecule's acceleration in the physisorption well, which leads to increased energy transfer from these vibrations to motion along the reaction path (see Figure S3 in the SI of Ref. [24]).

Our results point to the following promising approach to simulating heterogeneously catalyzed processes where elementary dissociative chemisorption reactions are rate controlling. First, perform AIMD calculations and molecular beam measurements of dissociative chemisorption on a low index face of the cat-

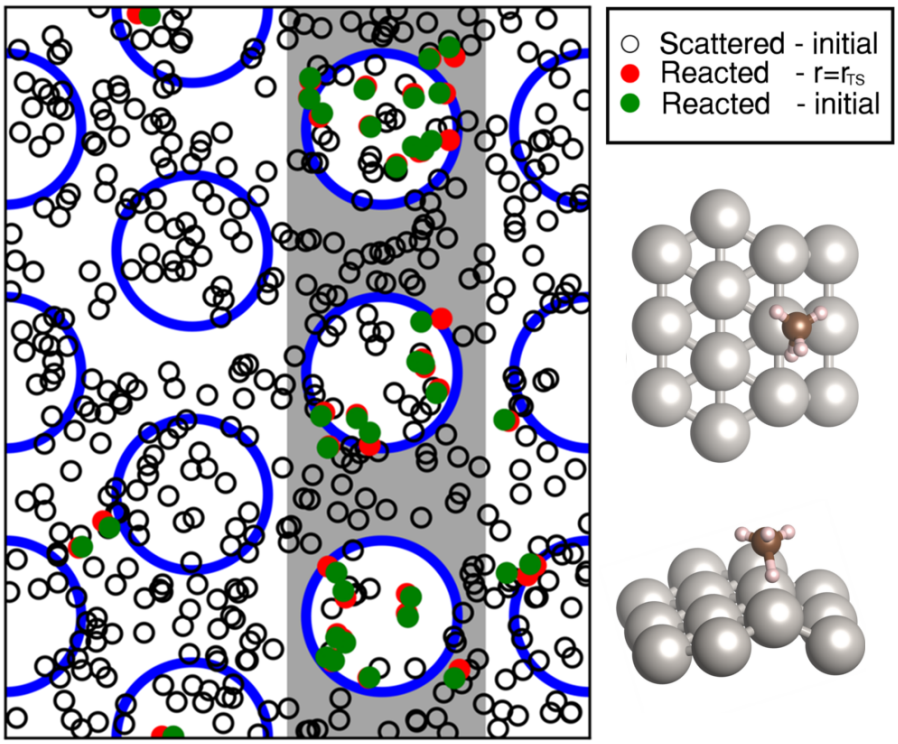

Figure 4.4: Points of impact of $CHD_3(\nu_1 = 1)$ molecules that react on Pt(211) for $\langle E_i \rangle = 69$ kJ/mol, at time zero (green circles) and at the time of reaction (red circles), and initial points of impact of the molecules that scatter (white circles). The blue circles denote the top layer Pt atoms and the grey zone consists of the step edge atoms where the molecules react predominantly. The top and side views of the minimum barrier geometry, which is located on a step edge atom, are reported as insets.

alyst metal to derive an SRP functional. Next, exploit the transferability of the SRP functional demonstrated here (between Pt(111) and Pt(211)) to simulate the overall reaction proceeding on multifaceted catalyst particles on which point and extended surface defects are also present. The SRP functional is then used to also compute barriers (or activation energies) at these defects, and at other low index facets (the transferability of SRP functionals among low index faces of metals was already demonstrated for H_2 + Cu(111) and Cu(100) [8]). Such an approach can help bridge the materials gap between surface science (which deals with smooth surfaces) and catalysis (with reactions typically proceeding over nanoparticles exhibiting defects) [42, 43]. The present research describes a test-case of transferability in which a single σ-bond is broken, for which the transition state typically occurs over a surface atom, and surface defects promote the reaction by decreasing the coordination of the surface atoms [44]. While the transferability is here demonstrated for only one example, arguments based on the dependence of the molecular adsorption energy on the co-ordination of the metal atom adsorbed to, experiments, and transition-state scaling relations suggest that the demonstrated transferability should hold more generally for σ-bond breaking (more details are reported in the next Section).

An additional structural requirement (high coordination of the transition state [44]) needs to be met for defect sites at which double or triple π-bonds are broken. Further investigations will therefore have to test whether the transferability found here for σ-bond breakage also holds when double and triple π-bonds are broken, as we believe. This belief can be supported on the basis of transition-state scaling relations also holding for the breaking of double and triple bonds (more details are reported in the next Section). Future investigation might also test whether our approach can be extended to deal with direct support effects on the catalysis (i.e., other than the effect that the support may alter the size distribution and the shape of the supported nanonparticles), and the presence of dopant atoms and additives [3]. Finally, on the basis of accurate quantum Monte-Carlo calculations on H_2 + Cu(111) [45] we anticipate that it will soon be possible to fit accurate SRP functionals to reliable QMC calculations on molecules reacting on surfaces.

This will put SRP-DFT on a first principles basis, and will yield a method that is easier to apply than the combined experimental/theoretical approach presented.

4.3.2 Implications for Simulating Heterogeneous Catalysis

The transferability of SRP functionals shown here for dissociative chemisorption of a molecule on a low-index, flat surface to a stepped surface points to a promising approach for accurately simulating rates of heterogeneously catalyzed reactions over metal nanoparticles. In this approach, one would use the finding that usually only a few states (transition states, or states describing adsorbed reactants, adsorbed reaction intermediates, or adsorbed products) exhibit a large degree of rate control [5]. Only for these states should it be necessary to determine the molecule-metal surface interaction energy accurately [5]. Of these states, accurate calculations of the transition states should be most important, as molecular adsorption energies are reasonably accessible through experiments using single crystal adsorption calorimetry and thermal desorption spectroscopy [46, 47]. It should be possible to fit a semi-empirical functional with an expression similar to that of Equation 4.1 to a molecule or reaction intermediate adsorbed on a low index metal surface either using existing experimental information, or in a procedure involving a new adsorption experiment. We argue that the transferability observed in the present work for transition states then suggests that the semi-empirical functional determined in this fashion should also accurately predict adsorption at surface defects, such as steps, edges, kinks and corners. Strong supporting evidence comes from recent work by Sautet and co-workers which showed that adsorption energies of OH and OOH on Pt [48] and other transition metal [49] surfaces depends linearly on the generalized coordination number of the surface atom these species adsorb to, and the finding that, based on these relations, theory is able to correctly predict that specific stepped Pt surfaces are more active for oxygen reduction than the Pt(111) surface [50].

The reaction studied in the present work is an important representative of a class of structure sensitive reactions in which the bond broken is a single σ-type bond (e.g., a CH or single CC bond) [44]. In the transition state of such reactions,

the dissociating molecule usually sits on top of a surface atom [44] (a "top site" if the reaction occurs on a low index surface). Usually, the reaction barrier is lowered over surface atoms of lower coordination number [44] (surrounded by fewer nearest neighbour metal atoms), for instance over surface atoms at the top edge of a step, as observed here for CHD_3 + Pt(211). The implication of our present work and earlier work on transferability among metal facets [8] is that one can use an SRP functional developed for the reaction on a low index surface to accurately compute barrier heights for the molecule's dissociation over surface atoms occurring in other low index facets and at surface line and point defects with lower coordination numbers of surface atoms. The derived barrier heights can then be used in kinetics simulations of the overall heterogeneously catalyzed reaction as it occurs over a metal nanoparticle exhibiting specific facets, line defects, and point defects. We argue that the rates calculated in this manner should be more accurate than rates calculated on the basis of standard density functionals (non-empirical functionals based on constraints, or conventional semi-empirical functions fitted to a range of chemical properties and/or materials properties [3]).

The above argument that rates over defected surfaces computed from SRP functionals accurately describe transition state energies on flat surfaces also has a basis in the recent work of Sautet and co-workers, and the so-called transition state scaling relationships. As noted above, it is already possible with standard functionals to predict which Pt crystal surface (with atoms located at defects possessing specific generalized coordination numbers) is most active for a specific reaction (oxygen reduction [50]). The adsorption energies of involved reactant molecules depend linearly on the generalized coordination number [48]. In turn, transition state energies usually scale linearly with the adsorption energies of reactants (the transition state scaling relationship) [1, 51]. The above suggests that transition state energies should scale linearly with generalized coordination numbers, and that if the off-set of the linear relationship is accurately determined (by determining the transition state energy for the flat surface) it should be possible to accurately determine the transition state energy for other generalized coordination numbers (on stepped surfaces) accurately as well.

Another class of structure-sensitive reactions, in which a double or triple π-bond breaks in the molecule, may present a greater challenge to transferability. Examples of such reactions are CO and N_2 bond breaking, where an additional requirement of the transition state (additional to presenting surface atoms with lower coordination number) is that the reaction site is able to coordinate many surface atoms to the dissociating molecule, to facilitate the breaking of a strong double or triple bond [44]. A well-known example concerns ammonia production over Ru particles, in which the rate limiting step is N_2 bond breaking. Nørskov and co-workers have established that this reaction is accelerated by so-called B5-sites, in which the dissociation molecule is co-ordinated by 5 surface atoms [17]. Incidentally, such B5 sites are also present at the Pt(211) steps, and, more generally, at surfaces where hcp(0001) terraces or fcc(111) terraces are connected by (100)-type steps (see Ref. [52] and Figure 1 therein). Our present results show that on Pt(211) methane reacts at the step edge sites that are part of these B5 sites. The additional requirement of providing a higher coordination to the dissociating molecule might be perceived to present a greater challenge to the transferability of SRP functionals. However, we emphasize that the difference between the two broad classes of structure sensitive reactions is gradual. In the case we have looked at, the SRP functional is able to accurately describe the effect of changing the coordination number of the surface atom above which dissociation occurs. In the case of double or triple bond breaking, the SRP functional should additionally be able to describe the effect of the coordination to additional surface atoms for transferability to hold. While the accuracy with which this can be done has yet to be established, we argue that a similar approach to that taken here for CHD_3 + Pt(111) and Pt(211) and based on an SRP functional for the flat surface should be better than simply taking a constraint-based or conventional semi-empirical functional to obtain reaction barrier heights on facets and at surface defect reaction sites. In this respect, it is encouraging that the transition scaling relations accurately describe the relation between the transition state energies of N_2, CO, and NO on fcc(211) surfaces and the adsorption energies of these molecules at the upper terrace hcp sites [53].

Finally, the question might arise whether the approach we advocate would be sensible if, for example, simple bond breaking of a reactant molecule dominates the reaction at steps, while the breaking of this bond is preceded by reaction with another reactant on the terraces. A practical example is the initiation of Fischer-Tropsch synthesis over $\approx$ 4.6 nm Co nanoparticles, which expose 15% under-coordinated sites, which are mostly step edges of A- and B-type capable of direct CO-dissociation [54]. For this example, Westrate *et al.* [54] concluded that one can reasonably assume that direct CO dissociation at the undercoordinated sites is the primary mechanism for the initiation of the Fischer-Tropsch reaction, even though the reaction on the facets might proceed through a mechanism in which CO is hydrogenated prior to CO bond breaking. Therefore, the development of an SRP functional for dissociative chemisorption of the CO molecule on a terrace and its application to the reaction of the same molecule at steps might help to accurately describe an overall catalyzed reaction if this reaction is dominated by the steps, even though the rate limiting step, and indeed the mechanism of the catalyzed reaction, could be different on the flat surfaces making up the facets. Here, by the overall catalyzed process we mean the initiation of a Fischer-Tropsch synthesis reaction, and not necessarily the complete Fischer-Tropsch reaction making higher hydrocarbons. Note that one can determine whether line defects (such as steps) or point defects (such as kinks) dominate the rate of a catalyzed process over catalyst particles by determining the degree of structure reactivity parameter α, which describes the dependence of the rate on the catalyst particle diameter d [55]. For example, $\alpha = 1$ describes a process where the rate is dominated by line defects, and this value was found to accurately describe the rate of steam reforming over supported Pt nanoparticles [19].

The above finding of $\alpha = 1$ for steam reforming over Pt nanoparticles is only one reason that steam reforming over Pt nanoparticles should constitute an ideal test case for our SRP density functional for methane interacting with Pt particles. Wei and Iglesia also found that steam reforming rates over Pt particles were exclusively limited by the first CH bond cleavage [19]. Additionally, they found that steam reforming over supported Pt nanoparticles proceeds over

essentially uncovered catalyst particles, and that support effects are indirect (they are described fully by how the support affects the shape of the catalyst particles).

Our approach is useful for getting accurate transition states for elementary dissociation reactions of molecules that are stable in the gas-phase, and therefore useful for simulating heterogeneous catalysis if such reactions play an important role in the mechanism of the catalyzed reaction. Examples of such reactions are dissociative chemisorption of methane in steam reforming [18, 19], of water in the water gas shift reaction [56], of N_2 in ammonia production [17, 57], and of CO in many realizations of the Fischer-Tropsch process [58]. It is less useful if the rate limiting step is, for instance, the hydrogenation of an already adsorbed reaction intermediate, as is the case for the overall Fischer-Tropsch synthesis reaction over supported Fe nanoparticles [59]. Catalyzed reactions with complex reaction mechanisms (such as hydrogenation of olefins on supported Pd catalysts involving sub-surface hydrogen [60]) certainly exist for which the present approach will be of little help. Nevertheless, our new approach is likely to provide valuable input for catalyzed reactions in which the overall rate is dominated by simple dissociation reactions of stable molecules.

4.4 Summary and Conclusions

We have demonstrated a joint theoretical-experimental approach (which we call reaction barriometry) that uses results from a reaction on a flat, low index metal surface to obtain a chemically accurate barrier for the same reaction on a stepped surface of the metal. We have applied a surface science approach to derive a semi-empirical functional that accurately describes the dissociation of CHD_3 on Pt(111), and then have shown the transferability of this functional to describe its dissociation on the stepped Pt(211) surface. Our approach can help bridge the materials gap between fundamental surface science studies on regular surfaces and real-life heterogeneous catalysis where reactions often proceed over defected metal nanoparticles.

Bibliography

[1] A. J. Medford, A. Vojvodic, J. S. Hummelshøj, J. Voss, F. Abild-Pedersen, F. Studt, T. Bligaard, A. Nilsson, and J. K. Nørskov, "From the Sabatier Principle to a Predictive Theory of Transition-Metal Heterogeneous Catalysis," *J. Catal.*, vol. 328, pp. 36–42, 2015.

[2] A. J. Medford, J. Wellendorff, A. Vojvodic, F. Studt, F. Abild-Pedersen, K. W. Jacobsen, T. Bligaard, and J. K. Nørskov, "Assessing the Reliability of Calculated Catalytic Ammonia Synthesis Rates," *Science*, vol. 345, pp. 197–200, 2014.

[3] M. K. Sabbe, M. F. Reyniers, and K. Reuter, "First-Principles Kinetic Modeling in Heterogeneous Catalysis: an Industrial Perspective on Best-Practice, Gaps and Needs," *Catal. Sci. Technol.*, vol. 2, pp. 2010–2024, 2012.

[4] G. Ertl, "Primary Steps in Catalytic Synthesis of Ammonia," *J. Vac. Sci. Technol. A*, vol. 1, pp. 1247–1253, 1983.

[5] C. Stegelmann, A. Andreasen, and C. T. Campbell, "Degree of Rate Control: How Much the Energies of Intermediates and Transition States Control Rates," *J. Am. Chem. Soc.*, vol. 131, pp. 8077–8082, 2009.

[6] C. A. Wolcott, A. J. Medford, F. Studt, and C. T. Campbell, "Degree of Rate Control Approach to Computational Catalyst Screening," *J. Catal.*, vol. 330, pp. 197–207, 2015.

[7] G. J. Kroes, "Toward a Database of Chemically Accurate Barrier Heights for Reactions of Molecules with Metal Surfaces," *J. Phys. Chem. Lett.*, vol. 6, pp. 4106–4114, 2015.

[8] L. Sementa, M. Wijzenbroek, B. J. van Kolck, M. F. Somers, A. Al-Halabi, H. F. Busnengo, R. A. Olsen, G. J. Kroes, M. Rutkowski, C. Thewes, N. F. Kleimeier, and H. Zacharias, "Reactive Scattering of H_2 from Cu(100): Comparison of Dynamics Calculations Based on the Specific Reaction Parameter

Approach to Density Functional Theory with Experiment," *J. Chem. Phys.*, vol. 138, p. 044708, 2013.

[9] E. Nour Ghassemi, M. Wijzenbroek, M. F. Somers, and G. J. Kroes, "Chemically Accurate Simulation of Dissociative Chemisorption of D_2 on Pt(111)," *J. Chem. Phys. Lett.*, vol. 683, pp. 329–335, 2017.

[10] F. Nattino, D. Migliorini, G. J. Kroes, E. Dombrowski, E. A. High, D. R. Killelea, and A. L. Utz, "Chemically Accurate Simulation of a Polyatomic Molecule-Metal Surface Reaction," *J. Phys. Chem. Lett.*, vol. 7, pp. 2402–2406, 2016.

[11] C. Díaz, E. Pijper, R. A. Olsen, H. F. Busnengo, D. J. Auerbach, and G. J. Kroes, "Chemically Accurate Simulation of a Prototypical Surface Reaction: H_2 Dissociation on Cu(111)," *Science*, vol. 326, pp. 832–834, 2009.

[12] H. S. Taylor, "A Theory of the Catalytic Surface," *Proc. R. Soc. Lond. A*, vol. 108, pp. 105–111, 1925.

[13] T. Zambelli, J. Wintterlin, J. Trost, and G. Ertl, "Identification of the "Active Sites" of a Surface-Catalyzed Reaction," *Science*, vol. 273, pp. 1688–1690, 1996.

[14] B. Hammer, "Bond Activation at Monatomic Steps: NO Dissociation at Corrugated Ru(0001)," *Phys. Rev. Lett.*, vol. 83, pp. 3681–3684, 1999.

[15] A. T. Gee, B. E. Hayden, C. Mormiche, A. W. Kleyn, and B. Riedmüller, "The Dynamics of the Dissociative Adsorption of Methane on Pt(533)," *J. Chem. Phys.*, vol. 118, pp. 3334–3341, 2003.

[16] F. Abild-Pedersen, O. Lytken, J. Engbæk, G. Nielsen, I. Chorkendorff, and J. K. Nørskov, "Methane Activation on Ni(111): Effects of Poisons and Step Defects," *Surf. Sci.*, vol. 590, pp. 127–137, 2005.

[17] K. Honkala, A. Hellman, I. N. Remediakis, A. Logadottir, A. Carlsson, S. Dahl, C. H. Christensen, and J. K. Nørskov, "Ammonia Synthesis from First-Principles Calculations," *Science*, vol. 307, pp. 555–558, 2005.

[18] Y. Xu, A. C. Lausche, S. G. Wang, T. S. Khan, F. Abild-Pedersen, F. Studt, J. K. Nørskov, and T. Bligaard, "In Silico Search for Novel Methane Steam Reforming Catalysts," *New J. Phys.*, vol. 15, p. 125021, 2013.

[19] J. M. Wei and E. Iglesia, "Mechanism and Site Requirements for Activation and Chemical Conversion of Methane on Supported Pt Clusters and Turnover Rate Comparisons among Noble Metals," *J. Phys. Chem. B*, vol. 108, pp. 4094–4103, 2004.

[20] R. R. Smith, D. R. Killelea, D. F. DelSesto, and A. L. Utz, "Preference for Vibrational over Translational Energy in a Gas-Surface Reaction," *Science*, vol. 304, pp. 992–995, 2004.

[21] R. D. Beck, P. Maroni, D. C. Papageorgopoulos, T. T. Dang, M. P. Schmid, and T. R. Rizzo, "Vibrational Mode-Specific Reaction of Methane on a Nickel Surface," *Science*, vol. 302, pp. 98–100, 2003.

[22] B. L. Yoder, R. Bisson, and R. D. Beck, "Steric Effects in the Chemisorption of Vibrationally Excited Methane on Ni(100)," *Science*, vol. 329, pp. 553–556, 2010.

[23] D. R. Killelea, V. L. Campbell, N. S. Shuman, and A. L. Utz, "Bond-Selective Control of a Heterogeneously Catalyzed Reaction," *Science*, vol. 319, pp. 790–793, 2008.

[24] D. Migliorini, H. Chadwick, F. Nattino, A. Gutiérrez-González, E. Dombrowski, E. A. High, H. Guo, A. L. Utz, B. Jackson, R. D. Beck, and G. J. Kroes, "Surface Reaction Barriometry: Methane Dissociation on Flat and Stepped Transition-Metal Surfaces," *J. Phys. Chem. Lett.*, vol. 8, pp. 4177–4182, 2017.

[25] M. B. Lee, Q. Y. Yang, and S. T. Ceyer, "Dynamics of the Activated Dissociative Chemisorption of CH_4 and Implication for the Pressure Gap in Catalysis: A Molecular-Beam High-Resolution Electron Energy Loss Study," *J. Chem. Phys.*, vol. 87, pp. 2724–2741, 1987.

[26] A. C. Luntz and D. S. Bethune, "Activation of Methane Dissociation on a Pt(111) Surface," *J. Chem. Phys.*, vol. 90, pp. 1274–1280, 1989.

[27] S. Nave and B. Jackson, "Methane Dissociation on Ni(111): The Role of Lattice Reconstruction," *Phys. Rev. Lett.*, vol. 98, p. 173003, 2007.

[28] G. Kresse and J. Furthmüller, "Efficient Iterative Schemes for Ab Initio Total-Energy Calculations Using a Plane-Wave Basis Set," *Phys. Rev. B*, vol. 54, pp. 11169–11186, 1996.

[29] G. Kresse and D. Joubert, "From Ultrasoft Pseudopotentials to the Projector Augmented-Wave Method," *Phys. Rev. B*, vol. 59, pp. 1758–1775, 1999.

[30] B. Hammer, L. B. Hansen, and J. K. Nørskov, "Improved Adsorption Energetics Within Density-Functional Theory Using Rrevised Perdew-Burke-Ernzerhof Functionals," *Phys. Rev. B*, vol. 59, pp. 7413–7421, 1999.

[31] J. P. Perdew, K. Burke, and M. Ernzerhof, "Generalized Gradient Approximation Made Simple," *Phys. Rev. Lett.*, vol. 77, pp. 3865–3868, 1996.

[32] M. Dion, H. Rydberg, E. Schröder, D. C. Langreth, and B. I. Lundqvist, "Van der Waals Density Functional for General Geometries," *Phys. Rev. Lett.*, vol. 92, p. 246401, 2004.

[33] D. A. King and M. G. Wells, "Reaction Mechanism in Chemisorption Kinetics: Nitrogen on the {100} Plane of Tungsten," *Proc. R. Soc. Lond. A*, vol. 339, pp. 245–269, 1974.

[34] F. Nattino, H. Ueta, H. Chadwick, M. E. van Reijzen, R. D. Beck, B. Jackson, M. C. van Hemert, and G. J. Kroes, "Ab Initio Molecular Dynamics Calculations versus Quantum-State-Resolved Experiments on CHD_3+Pt(111): New Insights into a Prototypical Gas–Surface Reaction," *J. Phys. Chem. Lett.*, vol. 5, pp. 1294–1299, 2014.

[35] S. Nave, A. K. Tiwari, and B. Jackson, "Dissociative Chemisorption of Methane on Ni and Pt Surfaces: Mode-Specific Chemistry and the Effects of Lattice Motion," *J. Phys. Chem. A*, vol. 118, pp. 9615–9631, 2014.

[36] F. Nattino, D. Migliorini, M. Bonfanti, and G. J. Kroes, "Methane Dissociation on Pt(111): Searching for a Specific Reaction Parameter Density Functional," *J. Chem. Phys.*, vol. 144, p. 044702, 2016.

[37] J. Frenkel, "Theorie Der Adsorption Und Verwandter Erscheinungen," *Z. Phys.*, vol. 26, pp. 117–138, 1924.

[38] L. Chen, H. Ueta, R. Bisson, and R. D. Beck, "Quantum State-Resolved Gas/Surface Reaction Dynamics Probed by Reflection Absorption Infrared Spectroscopy," *Rev. Sci. Instrum.*, vol. 84, p. 053902, 2013.

[39] B. Jackson and S. Nave, "The Dissociative Chemisorption of Methane on Ni(100): Reaction Path Description of Mode-Selective Chemistry," *J. Chem. Phys.*, vol. 135, p. 114701, 2011.

[40] B. Jiang, R. Liu, J. Li, D. Q. Xie, M. H. Yang, and H. Guo, "Mode Selectivity in Methane Dissociative Chemisorption on Ni(111)," *Chem. Sci.*, vol. 4, pp. 3249–3254, 2013.

[41] X. J. Shen, Z. J. Zhang, and D. H. Zhang, "Communication: Methane Dissociation on Ni(111) Surface: Importance of Azimuth and Surface Impact Site," *J. Chem. Phys.*, vol. 144, p. 101101, 2016.

[42] G. A. Somorjai, R. L. York, D. Butcher, and J. Y. Park, "The evolution of Model Catalytic Systems; Studies of Structure, Bonding and Dynamics from Single Crystal Metal Surfaces to Nanoparticles, and from Low Pressure ($<10^{-3}$ Torr) to High Pressure ($>10^{-3}$ Torr) to Liquid Interfaces," *Phys. Chem. Chem. Phys.*, vol. 9, pp. 3500–3513, 2007.

[43] H. J. Freund, H. Kuhlenbeck, J. Libuda, G. Rupprechter, M. Bäumer, and H. Hamann, "Bridging the Pressure and Materials Gaps between Catalysis and Surface Science: Clean and Modified Oxide Surfaces," *Top. Catal.*, vol. 15, pp. 201–209, 2001.

[44] R. A. van Santen, "Complementary Structure Sensitive and Insensitive Catalytic Relationships," *Acc. Chem. Res.*, vol. 42, pp. 57–66, 2009.

[45] K. Doblhoff-Dier, J. Meyer, P. E. Hoggan, and G. J. Kroes, "Quantum Monte Carlo Calculations on a Benchmark Molecule–Metal Surface Reaction: H_2+Cu(111)," *J. Chem. Theory Comput.*, vol. 13, pp. 3208–3219, 2017.

[46] T. L. Silbaugh and C. T. Campbell, "Energies of Formation Reactions Measured for Adsorbates on Late Transition Metal Surfaces," *J. Phys. Chem. C*, vol. 120, pp. 25161–25172, 2016.

[47] J. Wellendorff, T. L. Silbaugh, D. Garcia-Pintos, J. K. Nørskov, T. Bligaard, F. Studt, and C. T. Campbell, "A Benchmark Database for Adsorption Bond Energies to Transition Metal Surfaces and Comparison to Selected DFT Functionals," *Surf. Sci.*, vol. 640, pp. 36–44, 2015.

[48] F. Calle-Vallejo, J. Tymoczko, V. Colic, Q. H. Vu, M. D. Pohl, K. Morgenstern, D. Loffreda, P. Sautet, W. Schuhmann, and A. S. Bandarenka, "Finding Optimal Surface Sites on Heterogeneous Catalysts by Counting Nearest Neighbors," *Science*, vol. 350, pp. 185–189, 2015.

[49] F. Calle-Vallejo, D. Loffreda, M. T. M. Koper, and P. Sautet, "Introducing Structural Sensitivity into Adsorption-Energy Scaling Relations by Means of Coordination Numbers," *Nat. Chem.*, vol. 7, pp. 403–410, 2015.

[50] F. Calle-Vallejo, M. D. Pohl, D. Reinisch, D. Loffreda, P. Sautet, and A. S. Bandarenka, "Why Conclusions from Platinum Model Surfaces Do Not Necessarily Lead to Enhanced Nanoparticle Catalysts for the Oxygen Reduction Reaction," *Chem. Sci.*, vol. 8, pp. 2283–2289, 2017.

[51] A. A. Latimer, A. R. Kulkarni, H. Aljama, J. H. Montoya, J. S. Yoo, C. Tsai, F. Abild-Pedersen, F. Studt, and J. K. Nørskov, "Understanding Trends in C–H Bond Activation in Heterogeneous Catalysis," *Nat. Mater.*, vol. 16, pp. 225–229, 2017.

[52] K. Reuter, C. P. Plaisance, H. Oberhofer, and M. Andersen, "Perspective: On the Active Site Model in Computational Catalyst Screening," *J. Chem. Phys.*, vol. 146, p. 040901, 2017.

[53] P. N. Plessow and F. Abild-Pedersen, "Examining the Linearity of Transition State Scaling Relations," *J. Phys. Chem. C*, vol. 119, pp. 10448–10453, 2015.

[54] C. J. Weststrate, P. van Helden, and J. W. Niemantsverdriet, "Reflections on the Fischer-Tropsch Synthesis: Mechanistic Issues from a Surface Science Perspective," *Catal. Today*, vol. 275, pp. 100–110, 2016.

[55] J. K. Nørskov, T. Bligaard, B. Hvolbæk, F. Abild-Pedersen, I. Chorkendorff, and C. H. Christensen, "The Nature of the Active Site in Heterogeneous Metal Catalysis," *Chem. Soc. Rev.*, vol. 37, pp. 2163–2171, 2008.

[56] J. Nakamura, J. M. Campbell, and C. T. Campbell, "Kinetics and Mechanism of the Water-Gas Shift Reaction Catalysed by the Clean and Cs-Promoted Cu(110) Surface: a Comparison with Cu(111)," *J. Chem. Soc. Faraday Trans.*, vol. 86, pp. 2725–2734, 1990.

[57] C. T. Campbell, "Future Directions and Industrial Perspectives Micro- and Macro-Kinetics: Their Relationship in Heterogeneous Catalysis," *Top. Catal.*, vol. 1, pp. 353–366, 1994.

[58] R. A. van Santen, A. J. Markvoort, I. A. W. Filot, M. M. Ghouri, and E. J. M. Hensen, "Mechanism and Microkinetics of the Fischer–Tropsch Reaction," *Phys. Chem. Chem. Phys.*, vol. 15, pp. 17038–17063, 2013.

[59] T. J. Okeson, K. Keyvanloo, J. S. Lawson, M. D. Argyle, and W. C. Hecker, "On the Kinetics And Mechanism of Fischer-Tropsch Synthesis on a Highly Active Iron Catalyst Supported on Silica-Stabilized Alumina," *Catal. Today*, vol. 261, pp. 67–74, 2016.

[60] H. J. Freund, N. Nilius, T. Risse, and S. Schauermann, "A Fresh Look at an Old Nano-Technology: Catalysis," *Phys. Chem. Chem. Phys.*, vol. 16, pp. 8148–8167, 2014.